PHYSICAL REVIEW B VOLUME 52, NUMBER 21 1 DECEMBER 1995-I

X-ray-absorption spectroscopy and n-body distribution functions in condensed matter. I. Theory

Adriano Filipponi*
Dipartimento di Fisica, Università degli Studi dell'Aquila, Via Vetoio, 67010 Coppito, L'Aquila, Italy

Andrea Di Cicco
Dipartimento di Matematica e Fisica, Università degli Studi di Camerino, Via Madonna delle Carceri, 62032 Camerino (MC), Italy

Calogero Renzo Natoli
Istituto Nazionale di Fisica Nucleare, Laboratori Nazionali di Frascati, Casella Postale 13, 00044 Frascati, Italy

(Received 13 April 1994; revised manuscript received 11 August 1995)

The general theoretical framework underlying the GNXAS multiple-scattering (MS) data-analysis method for x-ray absorption spectroscopy (XAS) is presented. The main approximations leading to the reduction of the many-body process in that of a photoelectron scattering in an effective potential are summarized. The methods available to expand the extended x-ray-absorption fine-structure $\chi(k)$ into physically meaningful terms are described. In particular, emphasis is given to the definition of the irreducible n-body signals $\gamma^{(n)}$ that can be calculated directly by means of linear combinations of continued fractions, or by using their respective multiple-scattering series. It is found that even for an infinite system the expansion of the $\chi(k)$ signal in terms of $\gamma^{(n)}$ has a better convergence rate than the MS series. Simple expressions for performing the configurational averages of the structural signals in the presence of thermal and structural disorder are derived. These can be used for the structural analysis of molecular, crystalline, or moderately disordered systems. It is shown that in the case of highly disordered systems the expansion in terms of the $\gamma^{(n)}$ signals is the natural framework for the interpretation of the XAS signal. General equations for the ensemble-averaged $\chi(k)$ signal as a function of a series of integrals over the n-body $n>2$ distribution functions g_n are provided and the possible use of advanced strategies for the inversion of the structural information is suggested.

I. INTRODUCTION

X-ray-absorption spectroscopy[1,2] (XAS) is a powerful structural technique that allows one to investigate the neighborhood of a photoabsorber atom embedded in a condensed medium. The absorption cross section above a deep core-level excitation threshold presents oscillations characteristic of the compound being examined, due to interference effects in the transition-matrix element, which in turn are related to a suitably projected density of the unoccupied electronic states.

The basic theory for XAS (Refs. 3–6) has been developed since the early 1970's, in connection with the rapid experimental advances stimulated by the advent of synchrotron radiation, in particular supporting the structural origin of the so-called extended x-ray-absorption fine structure (EXAFS).[7,8] The EXAFS structural signal is defined as the relative oscillation with respect to a smooth total atomic cross section σ_0^t normalized to the atomic cross section of the edge under consideration σ_0, i.e., $\chi(k)=[\sigma(E)-\sigma_0^t(E)]/\sigma_0(E)$, where $k=\sqrt{2m(E-E_e)}/\hbar$ is the modulus of the photoelectron wave vector (E_e being the threshold energy). On the basis of both experimental evidence and approximate theory it was first realized[7,8] that each atom at a given distance R contribute to $\chi(k)$ with an oscillating signal of the type $A(k)\sin[2kR+\phi(k)]$. This fact suggested the use of a Fourier transformation technique[7,8] to isolate the contributions from the successive coordination shells, in a way similar to the well established methods for inverting the information contained in the structure factor $S(k)$ from diffraction experiments of disordered systems. It was also realized that the amplitude $A(k)$ is characteristic of the backscattering atom while the dephasing term $\phi(k)$, which can be usually approximated with a linear function of k, is, to a high degree of accuracy, the sum of two independent functions associated with photoabsorber and backscatterer atoms, respectively. This fact, known as "amplitude and phase transferability,"[9] is also at the basis of the standard EXAFS data-analysis method.[1,2]

Due to the simplicity of the data-analysis method the EXAFS technique has become very popular in recent times and has found many applications ranging from chemistry to molecular biology, including obviously many liquid and solid-state problems in condensed-matter physics. Some applications have dealt also with very dispersed systems, where the atoms of interest are only present in traces, or have addressed dynamical effects with typical timescales of the order of the milliseconds. Among the main advantages of XAS as a structural tool, the atomic selectivity, which is an important feature for studying multicomponent systems, merits particular mention. The present paper is focused on another quite remarkable characteristic of XAS, namely its sensitivity to atomic arrangements involving more than two atoms at the same time.

The photoabsorption process can be schematized as follows: a primary probe, usually a high-energy x-ray photon, interacts with a particular atom embedded in a certain struc-

0163-1829/95/52(21)/15122(13)/$06.00

ture. Above the absorption threshold energy, the photon excites a deep core electron generating a photoelectron that acts as a secondary probe. The photoelectron belongs to a continuum state with a well defined energy and its wave function spreads out of the excited atom interacting strongly (through Coulomb interaction) with the surrounding matter. The effects of the presence of neighboring atoms in the absorption cross section can be calculated in a perturbative scattering scheme starting from the isolated atom. Due to the strong electron-atom coupling it is not sufficient to limit the expansion to single-scattering terms, but higher-order multiple-scattering (MS) terms, should be included. MS terms probe the simultaneous presence of several atoms around the photoabsorber, in other words they probe the n-particle distribution functions. This sensitivity makes the XAS a unique probe in condensed systems. MS effects are dominant in the low kinetic energy region corresponding to the x-ray-absorption near-edge structure (XANES). Indeed the XANES sensitivity to higher-order distribution functions was quite early recognized,[10,11] and exploited.[12,13]

The occurrence of MS in the EXAFS region has been for many years the subject of some scientific debate. Its presence was initially identified in collinear atomic configurations where MS is enhanced by the focusing effect of the central intervening atom.[3,14] A typical case is the fourth shell in the fcc structure which is exactly shadowed by the first.[3] It was early recognized that a spherical wave approach[15] is essential for the correct prediction of low-angle scattering effects and expression for MS contributions were derived by various groups.[12,16,17] The presence of MS signals severely limits the practical applicability of the standard method of data analysis,[1,2,8] founded indeed on the single-scattering theory. For this reason large efforts have been devoted, until relatively recent times, to minimize the importance of the MS contributions.[19,20] Nevertheless, strong MS effects were found in metal-carbonyl compounds $Me_n(\mathrm{CO})_m$ because of the collinearity of the metal-C═O bond,[16,21] and in metal-imidazole complexes[22] due to the nearly collinear geometries and the short distances in the imidazole ring. Recently even MS "superfocusing" effects were detected from chains of Fe-F-Fe-F-Fe in FeF_3.[23] MS was also revealed in open structures[24,25] and its importance for a correct second-shell analysis was recognized. The possibility of using MS for bond-angle determinations in condensed matter was addressed by various authors.[24–26] Computational difficulties stimulated the development of efficient algorithms for MS calculations.[18,27–29] Recently the MS theory in XAS has been reviewed.[30]

The need to account correctly for MS contributions has stimulated the development of sophisticated packages that allow us to perform EXAFS data analysis based on theoretical calculations. Three main packages have been developed by different groups that differ mainly in the way MS is introduced and in the treatment of configurational average effects. The EXCURVE package[31,32] was developed by the Daresbury research group on the basis of early theoretical advances[15,16,33] and was actually the first user-oriented package to be developed. An extensive application of polarized MS to the analysis of surface EXAFS has been recently performed[34] by this group. The other two packages are the GNXAS,[35,36] developed by our group, whose theoretical founding will be widely described in the present paper, and the FEFF package[37] developed by the Seattle group, that is mainly based on the fast separable approximation by Rehr and Albers.[27,38] Recent applications of the FEFF package, regarded the understanding of alkali halides and mixed ionic salts spectra[39] and antiferrodistorsive phase transitions in perovskites.[40]

The purpose of the present paper is to discuss in a thorough manner the theory underlying the GNXAS method of EXAFS data analysis. An accompanying paper,[41] hereafter referred to as II, is instead devoted to the discussion of the fitting procedure and contains a representative set of applications to prototypical molecular and crystalline systems. The GNXAS method[36] has been already applied to a large variety of systems. Initial applications included a-Si,[42,43] the $\mathrm{Os}_3(\mathrm{CO})_{12}$ carbonyl cluster,[44] tetrahedral molecules,[45] brominated hydrocarbon molecules,[46] and high-T_c cuprates.[47] A complete and updated list of references is given in II. The GNXAS approach was specifically developed to allow the treatment of single and MS effects in disordered structures. For this reason a central aspect of the theory resides in the connection between MS signals and n-body distribution functions. The possibility of deriving reliable short-range radial distribution function profiles from EXAFS data in liquid systems, directly comparable with diffraction results or molecular-dynamics simulations was demonstrated.[48–51] Moreover, the importance of taking proper account of MS contributions in EXAFS data analysis of disordered systems was proven in several applications regarding amorphous solids[43,52] and liquids.[50,53–55]

The paper is organized as follows. Section II presents the underlying theory divided for clarity in three subsections: Section II A gives a brief discussion on the effective model potential used for the calculation of the atomic phase shifts, Sec. II B introduces and discusses the usual MS expansion, whereas Sec. II C derives the related expansion in terms of irreducible n-body signals and presents suitable methods for their calculations. In Sec. III the general ideas underlying the cluster analysis in terms of structural n-body units are presented and the $\gamma_T(k)$ and $\eta(k)$ signals are defined. In Sec. IV the general theory for the configurational average of the structural signals is reviewed, and finally in Sec. V the case of disordered systems is treated with particular emphasis on the sensitivity of the XAS signal to three-body distributions.

II. THEORY

Without loss of generality we consider the problem of calculating the $\chi(k)$ for a model cluster which is relevant to the structure under investigation. The procedure can be divided into the following steps: (a) calculation of the model potential for the final-state photoelectron, ensuing the reduction of the photoabsorption many-body problem to an effective one-electron problem moving in an optical potential, (b) the calculation of the atomic phase shifts, (c) the signal calculation, and (d) the configurational average. The model signal can be eventually compared with the experiment and possibly subject to a refinement procedure as a function of the unknown structural parameters. In principle, the refinement should involve all of the last four steps, since a change of the geometry affects, in principle, also the model potential. In practice, however, provided that the starting model cluster is sufficiently close to the real structure, the effects of small changes in the geometry (mainly bond distances) is negligible on both potential function and phase shifts, consequently they can be calculated once and for all at the beginning of the simulation. It will be shown that this is possible also for the $\gamma_T(k)$ and $\eta(k)$ signals. As a consequence the structural refinement procedure can involve only the last step, reducing considerably the complexity of the procedure. A self-consistent check can be eventually performed to ascertain that the optimized geometry gives rise to phase shifts identical, within a prescribed tolerance, to the starting ones, otherwise the entire procedure can be repeated until self-consistency is reached. Theoretical details on the various steps are given below.

A. Model potential and cross section

In order to put things into the proper context it might be useful to give here a sketchy description of the reduction of the photoabsorption many-body problem into that of an electron moving in an effective optical potential. Under quite general conditions it is possible to write the total many-body absorption cross section $\sigma_{\text{tot}}(\omega)$ in the following way:

$$\sigma_{\text{tot}}(\omega)=\int_0^\infty \sigma(\omega-\omega')A_c(\omega')\,d\omega' = \sigma(\omega)|S(\omega)|^2, \tag{1}$$

where $\sigma(\omega)$ is the one-electron absorption calculated in an optical potential that takes into account both the extrinsic losses of the photoelectron in the final state and the transient potential due to the switching of the core hole, $A_c(\omega)$ represents the intrinsic excitation spectrum of the core hole, and $\hbar\omega$ is the photon energy. Equation (1) has a quite simple physical content, in that it simply states that the total absorption cross section is obtained by convoluting the single-electron spectrum with the probability function that a certain excitation energy remains in the system and is not available to the kinetic energy of the photoelectron. The function $A_c(\omega)$ is clearly normalized to one: consequently the areas under the total absorption spectrum and the single-particle spectrum are the same so that the quantity $|S(\omega)|^2$ defined in Eq. (1) is expected to be structureless and nearly unity to a first approximation, except for the presence of quantum structures due to particularly strong inelastic channels which, however, are sizable only near threshold and in systems with high electron-electron correlation.

Under these assumptions the main problem becomes the construction of the effective optical potential and the solution of the associated Green's-function equation for the calculation of the one-electron cross section. Unfortunately, even this simpler problem is out of the reach of present day theoretical capabilities. In practice, in order to be able to cope in a simple way with the wide variety of systems usually encountered in practical applications, one tries to make a reasonable ansatz as to the nature of the optical potential so that it becomes applicable without too much difficulty to the various cases under study. Experience by several groups[32,36,56–58] has shown that the complex Hedin-Lundqvist (HL) potential,[59] suggested by Lee and Beni[5] for this type of problem provides a very good approximation to this kind of "universal" optical potential, at least for what concerns the extrinsic losses.[36,37,41,45,46] It represents substantially the self-energy of an electron embedded in a locally uniform interacting electron gas with a density equal to the local density of the system under study. Physically, this potential acts as a medium that diffracts the coherent electronic wave in the elastic channel by its real part and attenuates it via its imaginary part, giving rise to mean-free-path effects. The intrinsic losses are not accounted for in this approximation and neither is the attenuation of the electronic wave due to them. This is the reason why one keeps a constant many-body reduction factor S_0^2 (Refs. 37 and 61) for these excitations when fitting calculated signals to experimental data. The fitted values for this factor range from 0.85 to 0.90 in various materials indicating that the spectral weight of the intrinsic losses varies from 10 to 15% of the total. However, the reduction due to the extrinsic losses is automatically taken into account by using the complex HL potential. Notice that in this scheme one actually expects an energy dependence of S_0^2 near threshold, due to the progressive opening of successive inelastic channels with energy. Simulations using various theoretical models[56] have however shown that this energy dependence actually dies out quite rapidly beyond the first $40\approx 50$ eV above the rising edge, justifying in this way the use of a constant S_0^2 reduction factor in the energy range used for EXAFS analysis.

Coming back to the construction of the optical potential, one further notices that at given photoelectron energy the HL potential, as the Coulomb potential, depends only on the local density of the system so that a rapid and efficient way for generating such a density is required. This is obtained to a very good approximation by means of the Mattheiss prescription[60] which consists in overlapping neutral atomic charge densities. The relaxation of the charge density around the core hole and the screening of this latter are accounted for by taking for the photoabsorbing atom the self-consistent charge density relaxed around the core hole with the core electron promoted to the first empty orbital (cf the $Z+1$ atom approximation in Ref. 5). The ideal situation would be to have the self-consistent charge density of the system (photoabsorber plus surrounding) relaxed around the core hole and with the core electron promoted to the first empty valence state. This is sometimes essential very near the edge, but is less imperative in the energy region of EXAFS analysis.

Given the charge density and consequently the potential, a muffin-tin (MT) scheme is used to solve the Schrödinger equation for continuum states, whereby the potential is spherically averaged inside MT spheres around physical atoms, with radii chosen according to the Norman criterion,[62] and averaged to a constant in the interstitial region delimited by a convenient outer sphere enclosing the cluster under consideration.

Despite the apparently coarse approximations that are introduced in this way, the accuracy of the present scheme for the potential and phase-shift generation is sufficient, in the EXAFS region, to perform a reliable structural data analysis based on theoretical calculations. The main reason is that photoelectrons with kinetic energies greater than $E_k \sim 30$ eV are only weakly sensitive to the details of the effective potential. They are instead heavily scattered by the core regions of the atoms which are correctly described in the MT approximation. Also smoothing lifetime effects due to the imaginary part of the potential further limit this sensitivity. This circumstance justifies the development of advanced methods of data analysis focused on the possibility of extracting information on the many-atom distributions like the one presented in this paper.

Under the above assumptions and using the notation of Refs. 12 and 63, the polarization averaged XAS cross section for transitions to a dipole selected final state of angular momentum l_0 can be written as

$$\sigma(\omega)=\sigma_0\left[\Im\frac{1}{\Im(t_0^{l_0})}\frac{1}{2l_0+1}\sum_{m_0}\left[T(I-GT)^{-1}\right]_{0,0}^{L_0,L_0}\right]. \tag{2}$$

This equation is valid with good approximation for complex potential, whereas it is exact for real potential. For a more complete discussion on this point the reader is referred to Ref. 58. Here σ_0 is the atomic cross section, T and G are the atomic scattering and propagator matrices in a local basis. An element of one of these matrices is indicated by the indices i,j running over the different atomic centers in the structure, and by a further set of angular momenta L,L' (where $L=\{l,m\}$). Each couple of atomic indices identifies an "atomic" block of the matrices. In this representation the T matrix is block diagonal ($T_{i,j}=t_i\delta_{i,j}$) and, in the MT approximation for the potential, the scattering matrix for the atom at center i is diagonal in the L indices ($t_i^{L,L'}=t_i^l\ \delta_{L,L'}$), since the angular momentum is conserved in the scattering from a single site. As is well known, in terms of the lth potential phase shift δ_i^l at site i, one has $t_i^l=\exp(i\delta_i^l)\sin(\delta_i^l)$. These quantities are easily calculated by solving the Schrödinger equation for the potential at the corresponding site. It is worth noticing here that all MS equations, and in particular the XAS cross section (2), remains unaltered if one replaces the MT spheres with domains around each atom that do not leave any interstitial region (space filling cells), provided t^l is replaced by $t^{L,L'}$, taking in this way into account the nonspherical shape of the cell potential. Progress is being made along this direction, which will allow eventually the elimination of the MT approximation and hopefully the extension of the EXAFS analysis into the near-edge region.

The propagator matrix is instead composed of null diagonal blocks, (i,i) sites, and nonnull off-diagonal blocks $G_{i,j}^{L,L'}$ describing the free propagation from site i to site j $(i\neq j)$. The expression for a single propagator block involves $3J$ symbols and is given by

$$\begin{aligned}G_{i,j}^{L,L'}=&[4\pi(2l+1)(2l'+1)]^{1/2}\sum_{l_1}(2l_1+1)^{1/2}\\&\times\begin{pmatrix}l & l' & l_1\\0 & 0 & 0\end{pmatrix}\begin{pmatrix}l & l' & l_1\\m & -m' & m'-m\end{pmatrix}\\&\times(-1)^{m'}\ i^{l_1+1}h_{l_1}^{+}(kR_{ij})Y_{l_1,m'-m}(\hat{R}_{i,j}).\end{aligned} \tag{3}$$

Here h_l^+ are Hankel functions, $Y_{l,m}$ are the spherical harmonics, and $\vec{R}_{i,j}$ the vector joining site j to site i.

Equation (2) (or equivalent expressions) is at the basis of the XANES theory[11,58] that is commonly used to interpret the low-energy part of the absorption spectrum. An important consequence of the MS approach, whether in the MT approximation or not, is that the electronic and the structural part of the problem enter into the previous expressions in a decoupled way. All of the assumptions on the model optical potential for the excited electron are included in the scattering matrices t_i that are characteristic properties of the atomic sites i irrespective of their positions. Conversely, the matrices G_{ij} contain only information on the geometrical dispositions of atoms i and j irrespective of their actual scattering power.

From the preceding formulas it is clear that the relationship between geometry and signal is (unfortunately) strongly nonlinear. Indeed looking at Eq. (2) we observe that the G matrix appears in an inverse expression $(I-GT)^{-1}$ and for this reason the effects of different structural arrangements on the cross section can hardly be decoupled. The nonlinearity is the mathematical consequence of the strong coupling of the photoelectron with the surrounding atoms and it is the major reason responsible for the difficulty in analyzing XAS data. Most of the original results presented in this paper are related to a new way of tackling such a nonlinear problem. In the next section the traditional method for treating the inverse expression $(I-GT)^{-1}$, the so-called MS expansion, will be briefly reviewed.

B. Multiple-scattering expansion

Let us assume that the norm of the GT matrix, defined as the maximum modulus of its eigenvalues, is less then one, i.e., $||GT||<1$; in this case the formal matrix expansion $T(I-GT)^{-1}=T(I+GT+GTGT+GTGTGT+\cdots)$ is convergent and gives rise to the familiar MS series.[63] The above condition will certainly hold above a given energy since not only the elements of the G matrix decrease like $1/\sqrt{E}$ but also $||T||=\max|t_i|$ tends to zero much more rapidly with energy. The convergence threshold is system dependent, typical values range from below the edge to a few Ry. More stringent, however, for the practical use of the series is the condition that only a few terms be actually dominant.

By evaluating the diagonal terms corresponding to the photoabsorbing site and the final angular momentum in the formal power series and taking into account the block nature of the T and G matrices, the following expression is obtained:

$$\begin{aligned}\sigma(\omega)=\sigma_0\Bigg[&1+\sum_{i\neq 0}\chi_2^{0i0}+\sum_{\substack{i\neq j\\ i\neq 0,j\neq 0}}\chi_3^{0ij0}\\&+\sum_{\substack{i\neq j\neq k\\ i\neq 0,k\neq 0}}\chi_4^{0ijk0}+\cdots\Bigg],\end{aligned} \tag{4}$$

where the generic term is

$$\chi_n^{0i,\ldots,j0}=\Im\left(\frac{t_0^{l_0}}{\Im(t_0^{l_0})}\frac{1}{2l_0+1}\sum_{m_0}(\Xi^{0i,\ldots,j0})_{L_0,L_0}\right) \tag{5}$$

and specifically $\Xi^{0i0}=G_{0,i}t_iG_{i,0}t_0$ for χ_2^{0i0}, $\Xi^{0ij0}=G_{0,j}t_jG_{j,i}t_iG_{i,0}t_0$ for χ_3^{0ij0}, and Ξ^{0ijk0}

$=G_{0,k}t_kG_{k,j}t_jG_{j,i}t_iG_{i,0}t_0$ for χ_4^{0ijk0}. In this notation it is understood that the internal angular momentum indices have been saturated.

In the above expressions each term χ_n of the MS series can be related to a scattering path starting and ending at the origin with the constraint that successive sites must be distinct. Therefore the sums in the above expressions extend to all of the distinct sequences of sites of the type $0ijk,\ldots,pqr0$, with the constraint that i and r cannot be 0 and in general that any two successive indexes be different. Note that the "internal" sites $j,k,\ldots,p,q$ can be the origin again. The χ_n signals are oscillating functions of the type:

$$\chi_n(k)=A(k,R)\sin[kR_p+\phi(k,R)], \tag{6}$$

where A and ϕ are smooth functions of k and of the geometrical parameters R. The relevant frequency of the signal is determined by the path length R_p.

The relation between geometry and signal expressed in Eq. (4) is very cumbersome. The χ_2 terms probe the relative position of atoms 0 and i whereas χ_3 terms probe the positions of the atoms 0, i, and j and therefore they are sensitive to the two-particle and three-particle distribution, respectively. Starting with the χ_4 term the situation becomes more complicated, in fact, while the general $0ijk0$ probes four-particle correlations, special paths like $0i0k0$ or $0iji0$ and $0i0i0$ probe lower-order correlations (three-particle and two-particles, respectively). In general at order n, in χ_n there are paths involving all particle distributions from 2 to n if n is even or from 3 to n if n is odd. The symmetry properties of the successive terms of the MS series have been thoroughly investigated and efficient expressions for performing the actual calculations up to a large order in the scattering have been derived.[18]

The single-scattering approximation, valid in the high-energy limit, is obtained retaining only χ_2 terms in Eq. (4). In this case the signal is the sum of independent contributions from different surrounding atoms. The cross section depends only on the two-particle distribution, but, even more important, the relation between structure and signal is linearized, in the sense that the latter can be expressed as a linear functional of the radial distribution function.

It should be noted that if a further term (χ_3) is retained in Eq. (4) the linear relationship between structure an signal is not destroyed. The χ_3 term can be represented by a linear functional over the three-particle distribution. This circumstance is unfortunately of limited practical use because, in addition to χ_3 terms, higher-order terms (expecially χ_4) usually contribute with similar amplitudes and frequencies. Consequently, even with a path-length cutoff, higher-order terms in the MS series often have to be taken into account. In order to recast Eq. (4) into a linear functional form with respect to the distribution functions, a reordering of the MS terms is necessary. This often requires the inclusion of a very large number of terms with selection criteria that are not based anymore on the scattering order. In this respect the straightforward use of the MS series turns out to be rather cumbersome. For example, the FEFF package uses an *ad hoc* amplitude cutoff criterion in order to select the relevant MS paths to be considered in the calculations[38] and to cut down their prohibitively high number. In conclusion, there are drawbacks in the use of the traditional MS theory for the determination of structural many-body properties in condensed matter due to both convergence properties and cumbersome structure-signal relationship.

C. Expansion in terms of $\gamma^{(n)}$ signals

A different approach to the solution of the structural problem in Eq. (2) is based on a n-body decomposition of the cross section, which partially avoids the drawbacks related to the MS expansion. In general, it is always possible to calculate XAS cross sections associated with a cluster of N atoms. Let us indicate, as usual, the photoabsorber with "0" and the surrounding atoms with $i,j,k,\ldots$.

We define as the n-atom cross sections for increasing n the quantities:

(i) $\sigma(0)=\sigma_0$: atomic cross section;

(ii) $\sigma(0,i)$ cross section of the structure including atoms 0 and i only;

(iii) $\sigma(0,i,j)$ cross section of the structure including atoms 0, i and j;

(iv) $\sigma(0,i,j,k)$ cross section of the structure including atoms 0, i, j and k.

In the MT approximation these cross sections can be easily calculated using Eq. (2) including the appropriate number of atoms in the structure and therefore the appropriate number of blocks in the G and T matrices.

The irreducible n-body cross sections $\sigma^{(n)}(0,i_1,\ldots,i_{n-1})$ can be defined inductively starting from these quantities. For $n=2$ it is the contribution due to the presence of a second atom i that is given by

$$\sigma^{(2)}(0,i)=\sigma(0,i)-\sigma^{(1)}(0). \tag{7}$$

For $n=3$ the cross section for atoms 0, i, and j can be decomposed into the photoabsorber contribution, the two 0-i and 0-j two-body contributions, and an irreducible three-body contribution, that is given, by this definition as

$$\sigma^{(3)}(0,i,j)=\sigma(0,i,j)-\sigma^{(2)}(0,i)-\sigma^{(2)}(0,j)-\sigma^{(1)}(0). \tag{8}$$

Similarly the four-body contribution is given by

$$\begin{aligned}\sigma^{(4)}(0,i,j,k)=&\sigma(0,i,j,k)-\sigma^{(3)}(0,i,j)-\sigma^{(3)}(0,i,k)\\&-\sigma^{(3)}(0,j,k)-\sigma^{(2)}(0,i)-\sigma^{(2)}(0,j)\\&-\sigma^{(2)}(0,k)-\sigma^{(1)}(0).\end{aligned} \tag{9}$$

By induction, we can define the irreducible n-body contributions as

$$\begin{aligned}\sigma^{(n)}(0,i,j,\ldots,n)=&\sigma(0,i,j,\ldots,n)-\sum\sigma^{(n-1)}(0,S(n-2))\\&-\sum\sigma^{(n-2)}(0,S(n-3))-\cdots\\&-\sum_i\sigma^{(2)}(0,i)-\sigma^{(1)}(0),\end{aligned} \tag{10}$$

where $S(m)$ indicates a choice of m elements among $1,2\ldots N-1$ and the sums are extended to all possible choices.

Solving Eq. (10) for the total cross section $\sigma(0,i,j,\ldots,n)$ a useful expansion for this quantity in the n-body cross sections is obtained:

$$\sigma(0,i,j,\ldots,n)=\sigma_0+\sum_i \sigma^{(2)}(0,i)+\sum_{(i,j)} \sigma^{(3)}(0,i,j)+\sum_{(i,j,k)} \sigma^{(4)}(0,i,j,k)+\cdots+\sigma^{(n)}(0,i,j,\ldots,n). \qquad (11)$$

By introducing the dimensionless quantities $\gamma^{(n)}=\sigma^{(n)}/\sigma_0$, representing the irreducible n-body contributions to the EXAFS, Eq. (11) reduces to an equivalent expansion for the dimensionless experimental structural signal χ that differs substantially from the MS series (4):

$$\chi(0,i,j\ldots,n)=\sum_i \gamma^{(2)}(0,i)+\sum_{(i,j)} \gamma^{(3)}(0,i,j)+\sum_{(i,j,k)} \gamma^{(4)}(0,i,j,k)+\cdots+\gamma^{(n)}(0,i,j,\ldots,n). \qquad (12)$$

In this equation a linear relationship between structure (expressed in terms of 2, 3, 4, . . . n-body distributions) and signal is obtained. Equation (12) contains a finite number of terms if the system is finite (cluster) and becomes a series only in the case of a system with an infinite number of atoms. In this case it is expected anyway, due to mean-free-path effects, that the higher-order n-body terms are smaller than the lower-order ones and that the series has very good convergence properties.

The $\gamma^{(n)}$ signals are the central quantities in our approach, since they are associated with well precise n-body arrangements of the atoms. Two different methods for their calculation are available.

The first is based on the continued fraction expansions of the n-body cross sections.[28] Starting from Eq. (10) the two-body and the three-body contributions can be expressed in terms of total cross sections of clusters including two or three atoms only:

$$\gamma^{(2)}(0,i)=\sigma(0,i)/\sigma_0-1 \qquad (13)$$

and

$$\gamma^{(3)}(0,i,j)=\sigma(0,i,j)/\sigma_0-\sigma(0,i)/\sigma_0-\sigma(0,j)/\sigma_0+1. \qquad (14)$$

The $\sigma(0,i)$, $\sigma(0,j)$, and $\sigma(0,i,j)$ cross sections can be calculated using the previously published approach[28] that maps the inversion into a continued-fraction expansion. It has been shown that the continued-fraction approximants contain the exact terms of the MS series up to a given order, but in addition they include leading terms of the MS series to any order in the scattering. Convergence criteria can be derived in terms of the eigenvalues of the tridiagonal matrix generated by the recursion and conjectures can be formulated in terms of the eigenvalues of the $I-GT$ matrix which are less restrictive than the convergence conditions for the MS series. In particular the recursion algorithm is found to converge very rapidly for small clusters. Thus the $\gamma^{(n)}$ signals can be calculated directly using Eqs. (13) and (14) that reduce to a sum of continued fractions. This method of calculation of $\gamma^{(n)}$ signals has already been successfully used in several applications (see Ref. 41 and refs. therein).

The second method is based on the MS expansion for the $\gamma^{(n)}$. These can be derived in a direct way substituting in Eqs. (13) and (14) the respective MS series. For the two-body term (13), due to the two-blocks structure of the matrices, only even powers of TG give a contribution and the matrix expression results:

$$\left\{\begin{pmatrix} t_0 & 0 \\ 0 & t_i \end{pmatrix}\sum_{n=1}^{\infty}\left[\begin{pmatrix} 0 & G_{0,i} \\ G_{i,0} & 0 \end{pmatrix}\begin{pmatrix} t_0 & 0 \\ 0 & t_i \end{pmatrix}\right]^n\right\}^{0,0} = t_0G_{0i}t_iG_{i0}t_0+t_0G_{0i}t_iG_{i0}t_0G_{0i}t_iG_{i0}t_0+\cdots. \qquad (15)$$

The corresponding MS expansion, pictorially depicted in Fig. 1, results

$$\gamma^{(2)}(0,i)=\chi_2^{0i0}+\chi_4^{0i0i0}+\chi_6^{0i0i0i0}+\chi_8^{0i0i0i0i0}+\cdots. \qquad (16)$$

This kind of expansion has been used in early applications[36,43] and also its importance has been more recently emphasized by other authors[38] in conjunction with the appearance of shape resonances in the spectra of diatomic molecules (O_2 case discussed in Ref. 38). The number of MS terms required depends on k range, bond distance, and atomic numbers involved. In the EXAFS region, for short bonds terms up to χ_6 are found important whereas for longer bonds χ_4 is usually sufficient. The configurational average is also effective in the damping of these kind of higher-order MS signals. A peculiar feature in the MS expansion for $\gamma^{(2)}$ is that the successive terms have leading frequencies multiple of $2R$, R being the distance between atoms 0 and i. As a consequence there is a large frequency difference between the leading term χ_2 and the next order correction χ_4.

The MS series for $\gamma^{(3)}(0,i,j)$ can similarly be derived starting from Eq. (14):

FIG. 1. Pictorial view of the MS expansion for $\gamma^{(2)}$ signals, including terms up to χ_6. The $\gamma^{(2)}$ signals account for an infinite number of MS paths.

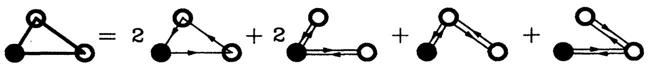

FIG. 2. Pictorial view of the MS expansion for $\gamma^{(3)}$ signals, including terms up to χ_4. The $\gamma^{(3)}$ signals account for an infinite number of MS paths.

$$\gamma^{(3)}=\Im\frac{1}{\Im(t_0^{l_0})}\left[\frac{1}{3}\sum_{m_0}\right]\left\{\begin{pmatrix} t_0 & 0 & 0\\ 0 & t_i & 0\\ 0 & 0 & t_j\end{pmatrix}\sum_{n=1}^{\infty}\left[\begin{pmatrix} 0 & G_{0i} & G_{0j}\\ G_{i0} & 0 & G_{ij}\\ G_{j0} & G_{ji} & 0\end{pmatrix}\begin{pmatrix} t_0 & 0 & 0\\ 0 & t_i & 0\\ 0 & 0 & t_j\end{pmatrix}\right]^n\right\}_{L_0,L_0}^{0,0}-\gamma_{0i}^{(2)}-\gamma_{0j}^{(2)}. \tag{17}$$

By performing the matrix products, in the three-body part, terms of any order in the scattering containing all three atoms 0, i, and j, or simply 0 and i or 0 and j are obtained. These last two contributions are however compensated exactly by the terms arising from the $\gamma^{(2)}$ signals appearing with negative sign. As a consequence $\gamma_{0,i,j}^{(3)}$ equals the sum of all possible MS signals involving "all and only" 0, i, and j in any possible sequence. The lowest order terms are the χ_3 signals corresponding to the sequences 0-i-j-0 and 0-j-i-0. Because of time-reversal symmetry the two signals coincide and only one of them can be considered with double degeneracy. This obviously occurs for all the paths that, when reversed, generate a different sequence. The sequences that are symmetric under inversion occur instead only once and have a single degeneracy.

By following the previous rules the MS expansion for the $\gamma^{(3)}$ signal is easily obtained:

$$\begin{aligned}\gamma^{(3)}=&2\chi_3^{0ij0}+2\chi_4^{0i0j0}+\chi_4^{0iji0}+\chi_4^{0jij0}+2(\chi_5^{0i0ij0}+\chi_5^{0j0ji0}+\chi_5^{0i0ji0}+\chi_5^{0j0ij0}+\chi_5^{0ijij0})+2\chi_6^{0i0i0j0}+2\chi_6^{0j0j0i0}+\chi_6^{0i0j0i0}\\ &+\chi_6^{0j0i0j0}+2\chi_6^{0i0iji0}+2\chi_6^{0j0jij0}+\chi_6^{0ijiji0}+\chi_6^{0jijij0}+2\chi_6^{0i0jij0}+2\chi_6^{0j0iji0}+2\chi_6^{0ij0ij0}+\chi_6^{0ij0ji0}+\chi_6^{0ji0ij0}+\cdots O(\chi_7)\cdots\end{aligned} \tag{18}$$

and depicted in Fig. 2. We point out that irrespective of the triangle geometry, the multiplicity of the possible paths brings a nearly continuous distribution of leading frequencies, for the successive χ_n terms, starting from $R_{0i}+R_{ij}+R_{j0}$. As a consequence $\gamma^{(3)}$ presents usually a regular oscillation in k space. Examples of the importance of χ_5 and χ_6 terms have been reported.[44] In most cases these higher-order terms contribute in the low-k range producing a detectable modification of the total signal.

By induction and using the definitions for the $\gamma^{(n)}$ signals (10) we find as a general rule that: the MS expansion for the $\gamma^{(n)}$ signal is given by the sum of the MS paths involving "all and only" the n atoms under consideration. All the other paths involving a minor number of atoms are indeed subtracted away by the $(n$-$m)$-body terms where $m=1,2,\ldots,n-2$ in (10). Obviously the lowest order paths will be of order n.

By applying the previous rule to the $\gamma^{(4)}$ signal, which depends on the position of the atoms 0, i, j, k, we obtain

$$\begin{aligned}\gamma^{(4)}=2[&\chi_4^{0ijk0}+\chi_4^{0ikj0}+\chi_4^{0kij0}+\chi_5^{0i0jk0}+\chi_5^{0i0kj0}+\chi_5^{0j0ik0}+\chi_5^{0j0ki0}+\chi_5^{0k0ij0}+\chi_5^{0k0ji0}+\chi_5^{0ijik0}+\chi_5^{0ikij0}+\chi_5^{0jijk0}+\chi_5^{0jkji0}\\ &+\chi_5^{0kikj0}+\chi_5^{0kjki0}+\chi_5^{0ijki0}+\chi_5^{0jikj0}+\chi_5^{0kijk0}+\cdots O(\chi_6)\cdots].\end{aligned} \tag{19}$$

The expressions becomes rapidly more cumbersome as the body order n is increased.

It is important to realize that while the MS expansions for the $\gamma^{(n)}$ have a meaning only in the case that the expansion relative to all the matrix inversions included in their definition converge (notice however that their convergence requirements are in general different from that relative to the matrix inversion of the whole cluster), the $\gamma^{(n)}$ signals always exist and can be calculated using the exact inversion.

In conclusion two methods are available for calculating the $\gamma^{(n)}$ signals: the first makes use of total cross-section calculations and continued-fraction expansions, the second consists in expanding the $\gamma^{(n)}$ signals in an appropriate MS series. Looking at expressions (16), (18), and (19), the advantage of incorporating in a few $\gamma^{(n)}$ signals a large (infinite) number of MS terms is evident. Such a way of associating MS signals is moreover also reasonable from the physical point of view. Indeed different MS term are not independent if they involve scattering processes on the same sets of atoms. From the computational point of view it should be noted however that, in the high-energy region, the continued-fraction expansion or other exact matrix inversion methods are time consuming due to the matrix size, while the MS series is faster because one can limit the calculation to a low scattering order. In this limit the MS calculation is preferable although the central quantities still remain the $\gamma^{(n)}$ signals.

Generally speaking the $\gamma^{(n)}$ signals are, like the χ_n [Eq. (6)], oscillating functions of the photoelectron wave-vector modulus k. The dominant frequency is that associated with the shortest path (i.e., lowest-order contribution) of the corresponding MS series. The oscillation shape has not necessarily a regular sinusoidal behavior because of the presence of higher harmonics. Indeed the MS terms associated with a γ signal provide a sort of frequency analysis of the γ signal itself that can be useful in several cases.

Finally we wish to address the question of the convergence of the expansion in $\gamma^{(n)}$ signals. Let us consider the two series expansions of the structural oscillation $\chi(k)$:

$$\chi(k)=\sum\chi_2+\sum\chi_3+\sum\chi_4+\cdots+\mathrm{Res}_{\chi}^{(n)} \tag{20}$$

$$\chi(k)=\sum\gamma^{(2)}+\sum\gamma^{(3)}+\sum\gamma^{(4)}+\cdots+\mathrm{Res}_{\gamma}^{(n)}. \tag{21}$$

Assuming that the MS series is absolutely convergent, then the remainder $\mathrm{Res}_{\chi}^{(n)}$ will satisfy the following inequality:

$$\mathrm{Res}_{\chi}^{(n)}=\sum_{i>n}\chi_i\leq\sum_{i>n}|\chi_i|<\infty. \qquad (22)$$

The remainder of the series (21) in the γ signals, for any given order will contain a smaller number of χ terms with respect to the remainder of the MS series, because many MS terms to any order are enclosed in the γ. As a consequence

$$\mathrm{Res}_{\gamma}^{(n)}=\sum_{i>n}\gamma^{(i)}\leq\sum_{i>n}|\gamma^{(i)}|\leq\sum_{i>n}|\chi_i|<\infty, \qquad (23)$$

and therefore also the series in the γ signals will be absolutely convergent. In general the rate of convergence of (21) is better (not worse) than the rate of the series (20).

III. CLUSTER ANALYSIS

In order to simulate the XAS signal of a given cluster using Eq. (12) it is necessary to perform an analysis of the main n-body configurations around the photoabsorber. Here only some general considerations will be made. Without loss of generality it can be assumed that there is only a single type of photoabsorber; this is the case of a single absorbing atom surrounded by atoms of different atomic number Z or the case in which there are many absorbers in equivalent positions. A sufficient condition for equivalence is that by means of spatial translations and rotations the absorber environments can be made to coincide atom by atom. In the following however we shall adopt a weaker definition, that is, two sites are equivalent if the n-body arrangements up to a given n and distance around the two sites coincide. The cutoff values for the distance and the order n can be set in such a way that all the relevant signals are reproduced. The case of the presence of more than one prototypical photoabsorber is a simple generalization of the case treated here.

The main, geometrically different, n-body configurations around a given atom 0, and their multiplicities, are identified by considering all the different arrangements involving couples of atoms (0, i), triplets of atoms (0, i, j), quadruplets of atoms (0, i, j, k), ... This is also done by introducing a natural, rotationally invariant, set of distances and angles that is associated in some unambiguous way to the configuration. In the case of a two-body configuration the only rotationally invariant coordinate is the distance $R_{0,i}$. In the case of a three-body configuration it is possible to use the two shortest distances among $R_{0,i}$, $R_{0,j}$, and $R_{i,j}$, and the angle in between (obviously different choices can be made as well). This choice is physically meaningful because the shortest bonds are, in general, real chemical bonds and the angle in between is a real bond angle. Using these coordinates, in addition, one should specify the photoabsorber position.

The case of the four-body configurations is a bit more complicated, indeed if one wishes to specify the geometry using three distances and three angles there are already two choices: either the three bonds are joined end by end forming a "chain" or they are bound to the same center, forming a "star." Criteria can be established, however, to make this choice unique. Again this variety reflects the different physical situations encountered when parametrizing, say, linear molecules or aggregates of atoms with a well-defined center.

Thus, each n-body structure will be defined by a set of coordinates, by the types of the atoms in the various positions, by the position of the photoabsorber, and by a characteristic dominant frequency, that is the length of the shortest path involving all of the atoms in the configuration. This characteristic frequency allows us to arrange the various n-body configurations in their "natural order." The most important configurations will be those associated with the lowest frequencies, that is, the two-body first-neighbor configuration with a length of $2R_b$. The most important three-body configuration will be associated with a frequency not smaller than $3R_b$, which would correspond to the equilateral triangle with three first-shell bonds as sides, but in many systems the shortest three-body path is much longer. Such a first three-body configuration will have, in general, a characteristic frequency comparable to the second or higher coordination shells (two-body configurations). In a similar manner higher-order n-body configurations will start contributing from successively higher frequencies certainly above nR_b. This circumstance is important, since by simple geometrical arguments it is possible to identify the frequency interval in which a given structure will contribute, and conversely by performing a frequency analysis of an experimental signal it is possible to select the relevant n-body configurations. Any experimental signal will show a natural upper frequency cutoff R_c, limited by experimental resolution or signal intensity, which will select automatically only a finite number of n-body structures. In particular also, the order of the maximum number of bodies involved will be finite and not larger than the integer part of R_c/R_b, but usually more stringent limits can be put using a more detailed knowledge of the structure under investigation. In conclusion, the signal given by Eq. (12) is actually dependent only on a limited number of distribution functions which can be easily identified and analyzed. In the interpretation of the signal of a completely unknown structure it is possible to make an *a priori* selection of the relevant n-body configurations thus limiting considerably the number of unknowns.

Coming back to the n-body analysis we observe that in a periodic structure (like a simple crystal) there will be an infinite number of equivalent photoabsorbers, thus a given n-body arrangement may contain m atoms (with $1\leq m\leq n$) of the photoabsorber atomic number. This atomic configuration will give rise to m different $\gamma^{(n)}$ terms in Eq. (12). In the $m>1$ case the signals will be generally different (apart from permutational symmetry). However, from the physical point of view they are not independent because they are associated with the same geometrical structure. Moreover, they have a similar frequency and can be described by the same structural parameters. As a consequence it is reasonable to group them together, in the spirit of reducing the independent components of $\chi(k)$, defining the total γ signals γ_T as

$$\gamma_T^{(n)}(i_1,i_2,\ldots,i_n)=\sum_{j}^{(i_j=0)}\gamma^{(n)}[i_j,\mathrm{Perm}(i_k,(k\neq j))], \qquad (24)$$

that is by the sum of all the related signals originating from the same structural arrangements of atoms $i_1,\ldots,i_n$ with the photoabsorber placed in any nonequivalent position. A pictorial view of the definition of the $\gamma_T^{(3)}$ signal for a general triangular configuration is given in Fig. 3. Examples of the cluster analysis in prototypical molecular and crystalline sys-

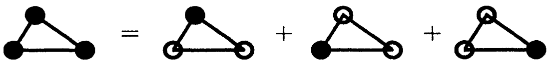

FIG. 3. Pictorial view of the definition of the total γ signal for a general triangular configuration of equivalent atoms.

tems will be given in II and the various details described here at a qualitative level will be further clarified.[41]

A different aspect of the cluster n-body analysis is highlighted by considering the hierarchical relationships between different peaks. A n-body configuration contains several $n-m$-body subconfigurations that are not independent. These considerations are particularly useful when the cluster analysis is focused on the successive coordination shells. The outer shell atoms will give rise to new two-body signals, but will also generate higher-order signals involving the atoms of the inner shells. Part of these signals will have approximately the same frequency because the dominant length is similar, therefore it is physically meaningful (in some cases) to associate them in an effective shell signal. Such a signal will be denoted by $\eta^{(n)}$ where n stands for the maximum number of atoms contributing together, i.e., the maximum index of a $\gamma^{(n)}$ signal, but clearly the signal

$$\eta^{(n)}=\gamma^{(n)}(\cdots)+\sum_{j=2}^{n-1}\gamma^{(j)} \tag{25}$$

will also contain contributions from smaller clusters. A typical example can be the second-shell contribution which usually gives rise to detectable three-body signal with a first-shell atom as the third atom. The three-body signal plus the two-body second-shell signal will be in this case the $\eta^{(3)}$ signal associated with the second shell. A pictorial view of the definition of the $\eta^{(3)}$ signal for a typical more distant shell is given in Fig. 4. From the previous considerations it appears that it may be useful sometimes to calculate n-body signals using the coordinates of a larger cluster including say $n+m$ bodies even though some of the coordinates will not affect the signal. In this way, by using the same set of coordinates for n-body and $n+m$-body signals, there is no need to introduce redundant structural parameters, thus limiting their total number.

Specific applications of this theory have been already published.[43–46,53,54] Moreover, a large number of examples of applications to the analysis of molecular and crystalline systems will be reported in II.

We end this section recalling that, unfortunately, the entire cluster analysis previously described becomes extremely complicated in the cases where the structure is highly disordered. In the limit of an N-atom cluster with no symmetry the number of two-body, three-body, and four-body configurations reaches the values of $N-1$, $(N-1)(N-2)/2!$, and $(N-1)(N-2)(N-3)/3!$, respectively. Selection criteria to account only for the dominant signals should be in this case applied. A further useful procedure, for low-symmetry structures, is to combine together several similar geometries and account for the additional structural disorder, that is present in addition to the thermal vibration effects. The ways to treat the effect of disorder are discussed in the following sections.

FIG. 4. Pictorial view of the definition of the $\eta^{(3)}$ signal associated with a typical distant (second) shell contribution.

IV. CONFIGURATIONAL AVERAGE OF THE SIGNALS

Different approaches are currently used to calculate the configurational damping of MS contributions. Early MS applications dealt with the difficulties of reproducing correctly the intensity of the signals. We have found that the approximation of an effective $\exp(-a^2k^2)$ damping term is sometimes inadequate. This is also due to the existence of spherical wave effects neglected in the simplest approaches whose analytic treatment is however quite involved.[64] The algorithm used in the GNXAS package is instead based on an advanced theory, that accounts for the correlated vibration of n-atom configurations[65] and spherical wave effects.

The effect of configurational disorder or thermal vibrations can be easily calculated in the case of small disorder, that is in the presence of a well defined (isolated) peak, not necessarily Gaussian, in the distribution function. This includes the thermal broadening of molecular or crystalline peaks as well as the case of small structural disorder. In the case of larger disorder, where the peaks are not any more well defined, but the distribution functions oscillate without vanishing in the configurational space, different average methods should be used as discussed in Sec. V.

MS signals $\chi_n(k)$, n-body signals $\gamma^{(n)}(k)$ or effective shell signals $\eta^{(n)}(k)$ can be treated in the same way. In all of these cases the signal, indicated generically by $\chi(k)$, can be written in terms of the amplitude $A(k,r)$ and phase $\psi(k,r)$ functions as

$$\chi(k)=\Im A(k,r)\exp[i\psi(k,r)], \tag{26}$$

where r indicates a set of geometrical coordinates which are sufficient to describe correctly the signal.

Let $P(r)$ be the normalized probability density describing a peak of the appropriate n-body distribution function. Configuration degeneracy (coordination number for $n=2$) is a trivial multiplicative factor and is omitted. The configurational average of the signal (26) over the peak distribution function $P(r)$ is given by

$$\langle\chi(k)\rangle=\Im\int dr A(k,r)\exp[i\psi(k,r)]P(r). \tag{27}$$

Because of the hypothesis of small disorder $P(r)$ will have a single modal value in position r_0 and will decrease rapidly to 0 for strongly distorted geometries. Therefore, in order to perform the integral in Eq. (27) it will be sufficient to know the signal in positions close to r_0. Because of the analytical dependence of the amplitude and phase functions on the geometrical parameters, it is possible to expand them in a Taylor series about the mean r_m of $P(r)$. Without loss of generality we can translate the origin of the r coordinates to this mean value. The expansions for amplitude and phase will then read

$$A(k,r)=A_0(k,r)|_{r=0}+(A_1(k,r)|_{r=0},r)+\frac{1}{2}(r,A_2(k,r)|_{r=0}r)+O(r^3), \tag{28}$$

$$\psi(k,r)=\psi_0(k,r)|_{r=0}+(\psi_1(k,r)|_{r=0},r)+\frac{1}{2}(r,\psi_2(k,r)|_{r=0}r)+O(r^3), \tag{29}$$

where $A_j(k,r)|_{r=0}$ (briefly A_j in the following) are the jth order derivatives with respect to all of the geometrical coordinates calculated for the mean r value. A similar notation has been used for the ψ functions, they are in general symmetric tensors of rank j. The symbol $(\cdots,\cdots)$ indicates summation over all coordinates. Obviously the approximation will be useful only if a low-order expansion is sufficient: in this case the derivatives can be easily calculated numerically by performing repeated calculations of the signal for slightly displaced geometries. This has turned out to be the most practical way because analytical approaches are much too involved. Equation (27) can be systematically approximated by

$$\langle\chi(k)\rangle=\Im\int dr\left[A_0+(A_1,r)+\frac{1}{2}(r,A_2r)+O(r^3)\right]\times\exp\left(i\left[\psi_0+(\psi_1,r)+\frac{1}{2}(r,\psi_2r)+O(r^3)\right]\right)P(r). \tag{30}$$

Isolating the zero-order terms in amplitude and phase as well as the leading linear term in the phase and writing the Taylor expansion for the amplitude as a differential operator with respect to ψ_1, which is the conjugated variables of r, we obtain

$$\langle\chi(k)\rangle=\Im A_0\exp(i\psi_0)\left[1+\frac{1}{iA_0}\left(A_1,\frac{\partial}{\partial\psi_1}\right)-\frac{1}{2A_0}\left(\frac{\partial}{\partial\psi_1},A_2\frac{\partial}{\partial\psi_1}\right)+O\left(\frac{\partial}{\partial\psi_1}^3\right)\right]\int drP(r)\exp[i(\psi_1,r)]\exp\left[\frac{i}{2}(r,\psi_2r)+O(r^3)\right]. \tag{31}$$

This is the most general expression for the damping of structural signals which occurs in the XAS case. Various terms can be easily identified: the initial factors before the large square bracket represent the undamped signal, the rest is a complex corrective factor. The amplitude expansion generates a differential operator, in square brackets, that acts on the last integral term. The integral, neglecting the last exponential term, i.e., neglecting ψ_2 and the successive terms in the phase expansion, is simply the characteristic function of the probability distribution $P(r)$. More specialized expressions can be derived, for specific $P(r)$ models and with the Taylor expansions truncated to some lower order.

In the limit of a δ-function-shaped $P(r)$, the corrective factor in Eq. (31) tends to 1 irrespective of A_1, A_2, ψ_1, and ψ_2, and $\langle\chi(k)\rangle$ equals the undamped signal. For small disorder the configurational average of the signal can be calculated including only the next term (usually the first-order one) in the Taylor expansions for both amplitude and phase. Special cases occur when a particular geometrical parameter has an extremum for the equilibrium configuration. Then the corresponding first derivatives vanish and the first nontrivial terms are the second-order derivatives. An example is given by a three-atom collinear configuration described by a 180° bond angle. Clearly the signal is affected in the same way by positive or negative angle displacements and therefore the Taylor expansion must be even in the angular coordinate.[44]

The possibility of using a low-order Taylor expansion is favored by the smoothness of the functions involved. In general both $\gamma^{(n)}$ and χ_n signals have rather smooth amplitude and phases, in a few cases, however, it is preferable to use the MS expansion for the $\gamma^{(n)}$. A typical example is that of $\gamma^{(2)}$; the higher harmonic χ_4 makes sometimes amplitude and phases of $\gamma^{(2)}$ slightly less smooth than the corresponding quantities in each χ_n term. In this case a high accuracy in the damping of $\gamma^{(2)}$ might require the inclusion of second-order terms, while a comparable accuracy can be obtained with first-order terms only, but considering the MS terms separately as $\chi_2+\chi_4+\cdots$. For $\gamma^{(n>2)}$ terms, as noted previously, the nearly continuous frequency spectrum of the various MS terms usually makes amplitude and phase rather smooth functions of the geometrical parameters. We have found that first order expansions are able to give accurate results in the case of thermal disorder in crystals or molecules, but also in several cases of configurational disorder in glasses and amorphous solids.

In the case where first-order derivatives are sufficient we obtain the following relevant expression:

$$\langle\chi(k)\rangle\sim\Im A_0\exp(i\psi_0)\left[1+\frac{1}{iA_0}\left(A_1,\frac{\partial}{\partial\psi_1}\right)\right]\Phi_c(\psi_1), \tag{32}$$

where $\Phi_c(\psi_1)$ indicates the characteristic function of the probability distribution calculated for argument ψ_1. Notice that for two-body contributions Equation (32) contains the usual results of the cumulant expansion, commonly applied for non-Gaussian terms. Eq. (32) can be further specialized in the case of particular probability distributions. In the fundamental case of Gaussian peaks (harmonic thermal disorder) $\Phi_c(\psi_1)=\exp[-1/2(\psi_1,M\psi_1)]$ where M is the covariance matrix of the Gaussian distribution, and (32) reduces to

$$\langle \chi(k)\rangle \sim \Im A_0 \exp(i\psi_0)\left[1+\frac{i}{A_0}(A_1, M\psi_1)\right] \times \exp[-1/2(\psi_1, M\psi_1)]. \tag{33}$$

For a generic three-body case the covariance matrix depends on six independent parameters

$$M=\begin{pmatrix} \sigma_1^2 & \sigma_{1,2}^2 & \sigma_{1,\theta}^2 \\ \sigma_{1,2}^2 & \sigma_2^2 & \sigma_{2,\theta}^2 \\ \sigma_{1,\theta}^2 & \sigma_{2,\theta}^2 & \sigma_\theta^2 \end{pmatrix}, \tag{34}$$

where the suffix 1, 2, and θ indicate first, second bond and angle, respectively. The diagonal parameters are the variances of the coordinates, while the off-diagonal terms express the correlation between bond-bond or bond-angle vibrations. Since the matrix must be positively defined, it is useful to define the dimensionless correlation parameters as $\rho_{ij}=\sigma_{ij}^2/\sqrt{\sigma_i^2\sigma_j^2}$ that satisfy $-1 \leq \rho \leq 1$. If $\rho=0$ then the bonds (or angles) vibrate in an independent manner, if $\rho=+1$, the fully correlated limit, both expand or contract at the same time, if $\rho=-1$ one expands when the other contracts and vice versa. In cases of particular symmetries the number of independent parameters is reduced. For an isosceles triangle where bonds 1 and 2 are equivalent $\sigma_1^2=\sigma_2^2$ and $\rho_{1,\theta}=\rho_{2,\theta}$ with four independent parameters. For an equilateral triangle parametrized with the length of the three equivalent bonds as coordinates there are only two independent quantities: bond variance σ_1^2 and correlation $\rho_{1,1'}$. Specific examples of covariance matrices will be discussed in II.

In the case of a two-body signal (say a χ_2 path) there is only one geometrical coordinate and M reduces to the single bond length variance σ^2, ψ_1 can be approximated by $2k$ and consequently the last exponential correction reduces to $\exp(-2k^2\sigma^2)$, the usual EXAFS Debye-Waller (DW) factor, while the correction in A_1 is usually small and neglected.

The previous equations (31), (32) generalize the common EXAFS DW correction to MS χ_n or $\gamma^{(n)}$ signals depending on a larger number of atoms. They are particularly efficient to be inserted in computational procedures and fitting routines.

V. DISORDERED SYSTEMS

In the case of disordered systems it is not anymore possible to have access to the exact positions of the atoms and information on the relative atomic positions is meaningful only in a probabilistic sense. For this reason the cluster analysis of Sec. III loses its relevance.

The fundamental microscopic observables are the n-body densities which are defined as appropriate ensemble averages.[66] For homogeneous and isotropic systems like liquids or amorphous solids, the n-particle densities depend only on translationally and rotationally invariant quantities. The one-particle density $\rho^{(1)}(r_1)=\rho$ equals the macroscopic density, $\rho^{(2)}(r_1,r_2)=\rho^2 g_2(|r_1-r_2|)$, and $\rho^{(3)}(r_1,r_2,r_3) =\rho^3 g_3(|r_{12}|,|r_{13}|,\phi)$. These expressions define the n-body distribution functions g_n.

The generalization of Eq. (12) to the case of a disordered system is obtained by substituting the sums over the n-particle configurations with integrals over the appropriate n-body distribution functions:

$$\langle \chi(k)\rangle = \int_0^\infty dr\ 4\pi r^2 \rho g_2(r)\gamma^{(2)}(r,k) + \int dr_1 dr_2 d\phi\ 8\pi^2 r_1^2 r_2^2 \sin(\phi)\rho^2 g_3(r_1,r_2,\phi)\gamma^{(3)}(r_1,r_2,\phi,k) + \int dr_1 dr_2 d\phi dr_3 d\Omega\ 8\pi^2 r_1^2 r_2^2 r_3^2 \sin(\phi)\rho^3 g_4(r_1,r_2,\phi,r_3,\Omega)\gamma^{(4)}(r_1,r_2,\phi,r_3,\Omega,k) + \cdots, \tag{35}$$

The integrals in the above expression formally extend to the whole coordinate space, however, because of the short-range nature of the kernels $\gamma^{(n)}$, they are actually limited to a region of linear dimensions of the order of few Å due to the exponential cutoff introduced by mean-free-path effects.

Equation (35) is the most general expression for the configurational average of the XAS signal in terms of the n-body distributions for a single component system. The relevance of the previously defined $\gamma^{(n)}$ signals appears obvious at this point, indeed they represent the kernels of the integral equation which links the structure to the observed signal. Equation (35) should be compared with the well-known expression for the static structure factor which can be measured by using x-ray or neutron diffraction:

$$S(k)=1+\frac{4\pi\rho}{k}\int_0^\infty (g_2(r)-1)r\sin(kr)dr. \tag{36}$$

Both $S(k)$ and the $\chi(k)$ provide one-dimensional information as a function of the variable k. The large difference in the kernels, however, makes the structural information on the $g_2(r)$ obtainable in the two cases largely complementary. In particular, while the $\chi(k)$ is extremely sensitive to the short-range order around the photoabsorber, but completely blind to atoms at distances above 6–8 Å (especially for disordered systems), the $S(k)$ data contain very important information also on the medium-range order of the systems. In addition the $S(k)$ obeys the compressibility sum-rule in the limit $k \rightarrow 0$. No analog for this exists for the $\chi(k)$. These topics have been discussed in some detail elsewhere.[49]

In spite of the complexity of the XAS kernels, which are not simple sine functions like in the $S(k)$ case, the present approximations in the XAS theory are sufficiently accurate to allow one to derive quantitative information from the analysis of a disordered structure.

The XAS presents advantages in the case of multicomponent systems because the signal depends only on the partial distribution functions relative to the photoabsorbing atom and often the spectra can be recorded at the edges of several components. However, the most important characteristic of the XAS signal is that, according to Eq. (35), it contains information on higher-order distributions which is of extreme interest. This information, contained in the second and successive integrals, is unique and characteristic of the XAS. At present there is no other direct experimental technique sensitive to the three-body and higher-order correlations in condensed matter. An indirect, widely used technique, proposed by Egelstaff, Page, and Heard[67] is based on the isothermal density derivative of the structure factor, a technique that can be applied to compressible systems in thermodynamic equilibrium, and has been widely applied in the case of noble gases and liquid metals. This approach however is based on the application of a sum-rule expression from which only average information on the $g^{(3)}$ is obtained. In comparison each particular geometrical configuration contributes to the EXAFS signal with a well defined frequency in k space which can be directly revealed.

In a series of recent papers[43,50,53,54] signals originating from the third-order integrals have been detected in several ordered or disordered condensed systems. A surprising circumstance is that in many cases the ratio between MS and single-scattering components may even increase with the disorder of the sample.

From these results it is clear that XAS can provide quantitative, easy to obtain, and unique information on three-body and higher-order distributions in condensed matter. Such information is of particular importance to test model interatomic interactions and simulation procedures, expecially in those cases where three-body and higher-order forces are important. These considerations are of central importance and motivate the efforts to understand the XAS signal in terms of distribution functions presented in this paper. We emphasize that the information contained in the $S(k)$ and the $\chi(k)$ signals are extremely complementary and any effort to combine the data should be encouraged.

Equation (35) is at the basis of our efforts to analyze heavily disordered systems like amorphous solids[43] and liquids.[48,50,53,54] The actual integral expression over the $g_2(r)$ function has been used to calculate the pair EXAFS signal associated with distribution functions obtained from diffraction experiments or molecular-dynamics simulations.[48,49,53] Using consistent $g_2(r)$ models and compressibility constraints it has been possible to refine by EXAFS analysis the short-range $g_2(r)$ shape in several liquid systems.[49,48,51] The three-dimensional integral over the g_3 distribution presents larger computational difficulties. A part of the integral coming from the main peak of the g_3 distribution in amorphous silicon has been used, for instance, to compare the structural signals associated with different available models in reproducing the observed EXAFS signal.[52,65] The use and present limitations of the application of Eq. (35) to prototypical systems will be discussed in paper II.[41]

For future developments in the field one might envisage the adoption of more sophisticated inversion algorithms, either based on regularized algorithms[68] or reverse Monte Carlo techniques.[69]

VI. CONCLUSIONS

The present paper provides a complete account of the theory underlying the GNXAS method for EXAFS data analysis. The central elements in our approach are the irreducible n-body signals $\gamma^{(n)}$. The EXAFS signal can be expanded in terms of $\gamma^{(n)}$ obtaining a very powerful decomposition into physically meaningful quantities. This expansion is found to have a better convergence rate than the MS series because each $\gamma^{(n)}$ signal accounts for an infinite number of MS terms. Direct ways for calculating the $\gamma^{(n)}$ signals, either in terms of continued-fraction expansions or via MS expansions, are described.

The GNXAS method of data analysis was specifically developed for a high flexibility and accuracy in the calculation of configurational averages. In the cases of molecular or crystalline systems, or in the presence of small configurational disorder, analytical expressions that generalize the Debye-Waller factor correction to $\gamma^{(n)}$ signals can be derived. General expressions for Gaussian or non-Gaussian cases are reported and discussed. In the case of highly disordered systems the present formalism provides an expression of the averaged signal in terms of a series of integrals over the n-body distribution functions $g^{(n)}(r \ldots)$. In this case the $\gamma^{(n)}$ play the role of the kernels of integrals. The possibility of using XAS experiments to probe local pair and higher-order correlations in disorder matter is addressed, current applications have been discussed, and possible directions of further developments suggested.

The present paper is intended to provide a self-contained reference for the basic theoretical ingredients of the GNXAS method. Specific examples and details about fitting approaches presently used in actual data analysis are described in the following paper II.[41]

---

[*] Present address: E.S.R.F., BP 220, F-38043 Grenoble Cedex, France.

[1] P. A. Lee, P. Citrin, P. Eisenberger, and B. Kincaid, Rev. Mod. Phys. **53**, 769 (1981); B. K. Teo and D. C. Joy, *EXAFS Spectroscopy, Techniques and Applications* (Plenum, New York, 1981); T. M. Hayes and J. B. Boyce, in *Solid State Physics*, edited by H. Eherenreich, F. Seitz, and D. Turnbull (Academic, New York, 1982), Vol. 37, p. 173.

[2] *X-ray Absorption: Principles, Applications, Techniques of EXAFS, SEXAFS, and XANES*, edited by D. C. Koningsberger and R. Prins (Wiley, New York, 1988).

[3] P. A. Lee and J. B. Pendry, Phys. Rev. B **11**, 2795 (1975).

[4] C. A. Ashley and S. Doniach, Phys. Rev. B **11**, 1279 (1975).

[5] P. A. Lee and G. Beni, Phys. Rev. B **15**, 2862 (1977).

[6] W. L. Schaich, Phys. Rev. B **27**, 4028 (1973).

[7] D. E. Sayers, E. A. Stern, and F. W. Lytle, Phys. Rev. Lett. **27**, 1204 (1971).

[8] E. A. Stern, D. E. Sayers, J. G. Dash, H. Shechter, and B. Bunker, Phys. Rev. Lett. **38**, 767 (1977); E. A. Stern, S. M. Heald, and B. Bunker, Phys. Rev. Lett. **42**, 1372 (1979).

[9] P. H. Citrin, P. Eisenberger, and B. M. Kincaid, Phys. Rev. Lett. **36**, 1346 (1976).

[10] P. J. Durham, J. B. Pendry, and C. H. Hodges, Solid State Commun. **38**, 159 (1981).

[11] P. J. Durham, in *X-ray Absorption: Principles, Applications, Techniques of EXAFS, SEXAFS, and XANES* (Ref. 2), p. 53.

[12] M. Benfatto, C. R. Natoli, A. Bianconi, J. Garcia, A. Marcelli, M. Fanfoni, and I. Davoli, Phys. Rev. B **34**, 5774 (1986).

[13] P. Kizler, Phys. Rev. Lett. **67**, 3555 (1991).

[14] B. K. Teo, J. Am. Chem. Soc. **103**, 3990 (1981).

[15] S. J. Gurman, N. Binsted, and I. Ross, J. Phys. C **17**, 143 (1984).

[16] S. J. Gurman, N. Binsted, and I. Ross, J. Phys. C **19**, 1845 (1986).

[17] R. V. Vedrinskii and L. A. Bugaev, J. Phys. (Paris) Colloq. **47**, C8-89 (1986).

[18] C. Brouder, M. F. Ruiz-López, R. F. Pettifer, M. Benfatto, and C. R. Natoli, Phys. Rev. B **39**, 1488 (1989).

[19] G. Bunker and E. A. Stern, Phys. Rev. Lett. **52**, 1990 (1984).

[20] C. E. Bouldin, G. Bunker, D. A. McKeown, R. A. Forman, and J. J. Ritter, Phys. Rev. B **38**, 10 816 (1988).

[21] R. F. Pettifer, in *Metal Clusters in Catalysis*, edited by B. C. Gates, L. Guczi, and H. Knozinger (Elsevier Science, Amsterdam, 1986), p. 254.

[22] R. W. Strange, N. J. Blackburn, P. F. Knowles, and S. S. Hasnain, J. Am. Chem. Soc. **109**, 7157 (1987).

[23] A. Kuzmin and Ph. Parent, J. Phys. Condens. Matter **6**, 4395 (1994).

[24] A. Bianconi, A. Di Cicco, N. V. Pavel, M. Benfatto, A. Marcelli, C. R. Natoli, P. Pianetta, and J. Woicik, Phys. Rev. B **36**, 6426 (1987).

[25] M. F. Ruiz-López, M. Loos, J. Goulon, M. Benfatto, and C. R. Natoli, Chem. Phys. **121**, 419 (1988).

[26] R. V. Vedrinskii, L. A. Bugaev, and I. G. Levin, Phys. Status Solidi B **150**, 307 (1988); Physica B **158**, 421 (1989).

[27] J. J. Rehr and C. R. Albers, Phys. Rev. B **41**, 8139 (1990).

[28] A. Filipponi, J. Phys. Condens. Matter **3**, 6489 (1991).

[29] A. Kuzmin and J. Purans, J. Phys. Condens. Matter **5**, 267 (1993).

[30] L. Fonda, J. Phys. Condens. Matter **4**, 8269 (1992).

[31] N. Binsted, J. W. Campbell, S. J. Gurman, and P. C. Stephenson, The Daresbury Laboratory EXCURVE90 program, Daresbury Laboratory, Warrington WA4 4AD, England.

[32] N. Binsted, J. W. Campbell, S. J. Gurman, and P. C. Stephenson, The Daresbury Laboratory EXCURVE92 program, Daresbury Laboratory, Warrington WA4 4AD, England.

[33] S. J. Gurman, J. Phys. C **21**, 3699 (1988).

[34] N. Binsted and D. Norman, Phys. Rev. B **49**, 15 531 (1994).

[35] The acronym GNXAS derives from g_n (the n-body distribution functions) and XAS (x-ray-absorption spectroscopy).

[36] A. Filipponi, A. Di Cicco, T. A. Tyson, and C. R. Natoli, Solid State Commun. **78**, 265 (1991).

[37] J. Mustre de Leon, J. J. Rehr, S. I. Zabinsky, and R. C. Albers, Phys. Rev. B **44**, 4146 (1991); J. J. Rehr, J. Mustre de Leon, S. I. Zabinsky, and R. C. Albers, J. Am. Chem. Soc. **113**, 5135 (1991).

[38] J. J. Rehr, R. C. Albers, and S. I. Zabinsky, Phys. Rev. Lett. **69**, 3397 (1992).

[39] A. I. Frenkel, E. A. Stern, M. Qian, and M. Newville, Phys. Rev. B **48**, 12 449 (1993); A. Frenkel, E. A. Stern, A. Voronel, M. Qian, and M. Newville, Phys. Rev. Lett. **71**, 3485 (1993); Phys. Rev. B **49**, 11 662 (1994).

[40] B. Rechav, Y. Yacoby, E. A. Stern, J. J. Rehr, and M. Newville, Phys. Rev. Lett. **72**, 1352 (1994).

[41] A. Filipponi and A. Di Cicco, following paper, Phys. Rev. B **52**, 15 135 (1995).

[42] A. Filipponi, A. Di Cicco, M. Benfatto, and C. R. Natoli, J. Non-Cryst. Solids **114**, 229 (1989).

[43] A. Filipponi, A. Di Cicco, M. Benfatto, and C. R. Natoli, Europhys. Lett. **13**, 319 (1990).

[44] A. Filipponi, A. Di Cicco, R. Zanoni, M. Bellatreccia, V. Sessa, C. Dossi, and R. Psaro, Chem. Phys. Lett. **184**, 485 (1991).

[45] A. Di Cicco, S. Stizza, A. Filipponi, F. Boscherini, and S. Mobilio, J. Phys. B **25**, 2309 (1992).

[46] E. Burattini, P. D' Angelo, A. Di Cicco, A. Filipponi, and N. V. Pavel, J. Phys. Chem. **97**, 5486 (1993).

[47] A. Di Cicco and M. Berrettoni, Phys. Lett. A **176**, 375 (1993).

[48] P. D' Angelo, A. Di Nola, A. Filipponi, N. V. Pavel, and D. Roccatano, J. Chem. Phys. **100**, 885 (1994).

[49] A. Filipponi, J. Phys. Condens. Matter **6**, 8415 (1994).

[50] A. Di Cicco and A. Filipponi, Europhys. Lett. **27**, 407 (1994).

[51] A. Filipponi and A. Di Cicco, Phys. Rev. B **51**, 12 322 (1995).

[52] A. Filipponi, F. Evangelisti, M. Benfatto, S. Mobilio, and C. R. Natoli, Phys. Rev. B **40**, 9636 (1989).

[53] L. Ottaviano, A. Filipponi, A. Di Cicco, S. Santucci, and P. Picozzi, J. Non-Cryst. Solids **156-158**, 112 (1993).

[54] A. Di Cicco and A. Filipponi J. Non-Cryst. Solids **156-158**, 102 (1993).

[55] A. Filipponi, P. D' Angelo, N. V. Pavel, and A. Di Cicco, Chem. Phys. Lett. **225**, 150 (1994).

[56] S.-H. Chou, J. J. Rehr, E. A. Stern, and E. R. Davidson, Phys. Rev. B **35**, 2604 (1987).

[57] Dan Lu and J. J. Rehr, Phys. Rev. B **37**, 6126 (1988).

[58] T. A. Tyson, K. O. Hodgson, C. R. Natoli, and M. Benfatto, Phys. Rev. B **46**, 5997 (1992).

[59] L. Hedin and B. I. Lundqvist, J. Phys. C **4**, 2064 (1971).

[60] L. F. Mattheiss, Phys. Rev. A **134**, 970 (1964).

[61] J. J. Rehr, E. A. Stern, R. L. Martin, and E. R. Davidson, Phys. Rev. B **17**, 560 (1978).

[62] J. G. Norman, Mol. Phys. **31**, 1191 (1976)

[63] C. R. Natoli and M. Benfatto, J. Phys. (Paris) Colloq. **47**, C8-11 (1986).

[64] C. Brouder, J. Phys. C **21**, 5075 (1988); C. Brouder and J. Goulon, Physica B **158**, 351 (1989).

[65] M. Benfatto, C. R. Natoli, and A. Filipponi, Phys. Rev. B **40**, 9626 (1989).

[66] J. P. Hansen and I. R. Mc Donald, *Theory of Simple Liquids* (Academic, New York, 1976).

[67] P. A. Egelstaff, D. I. Page, and C. R. T. Heard, J. Phys. C **4**, 1453 (1971).

[68] Y. A. Babanov and V. R. Shvetsov, J. Phys. (Paris) Colloq. **47**, C8-37 (1986); Y. A. Babanov, V. V. Vasin, A. L. Ageev, and N. V. Ershov, Phys. Status Solidi **105**, 747 (1981).

[69] S. J. Gurman and R. L. McGreevy, J. Phys. Condens. Matter **2**, 9463 (1990).